PHYSICAL REVIEW B VOLUME 30, NUMBER 11 1 DECEMBER 1984

Theory of domain growth in an order-disorder transition

Gene F. Mazenko
The James Franck Institute and Department of Physics, The University of Chicago, Chicago, Illinois 60637

Oriol T. Valls
School of Physics and Astronomy, University of Minnesota, Minneapolis, Minnesota 55455
(Received 19 January 1984)

We consider the growth of order in a two-dimensional Ising system with spin-flip dynamics (no conservation laws) quenched from above to below T_c. We use an iterative method, which allows for the interaction among many length and time scales, to calculate correlation functions in coordinate and Fourier space as a function of the time after quench. The method which we use to derive recursion relations is a reformulation of our previous work. We derive analytically scaling forms for the "Bragg peak" part of dynamic structure factor $\tilde{C}(\vec{q},t)$, the nearest-neighbor correlation function, the width of the central peak, q_w, and the maximum value of the peak. We evaluate the corresponding scaling functions. These scaling laws for the width and peak height are new and elucidate the role of the final temperature in the problem. In particular, we find that the peak height grows as $t^{7/8}$ for quenches to precisely T_c. Our results also show that the Cahn-Allen curvature-driven growth law, $q_w \sim t^{-1/2}$, is valid after relatively short times in this system. Our results agree quantitatively with Monte Carlo calculations in direct comparisons.

I. INTRODUCTION

This is a time of great progress in the development of our understanding of the kinetics of first-order phase transformations. Spurred on by the results of experiments and computer simulations,[1] we are beginning to see that these problems are governed by rules which are more general and ubiquitous than had previously been thought. Indeed, in problems involving rapid temperature quenches from disordered phases, we now understand that the physics at long times t is dominated by the existence of a single length, the average domain size, $L(t)$, which grows without bound as time proceeds after a quench. Because of this dominant length, the quasistatic structure factor satisfies a scaling law and it makes sense to consider the notion that the growth laws for $L(t)$ and the scaling functions may partition various physical systems into "universality" classes. We are still quite far from a complete understanding of the basis for the determination of these classes. There has been some progress in cataloging various possibilities. However, given the increasing interest and work on this problem, there has been little direct theoretical work which attempts to understand the origins of $L(t)$ and the subsequent establishment of scaling behavior.[2] Unlike the case of critical phenomena, where the dominant length is the correlation length, the average domain size does not naturally appear in any linearized process involving the competition of many length scales. It is because of the highly nonlinear origins of $L(t)$ that this problem is difficult from a theoretical point of view.

In previous papers[3,4] we showed how a renormalization-group (RG) method could be used to treat problems of nonlinear growth phenomena. In Ref. 3 [Mazenko and Valls (MV)] we considered the growth of order in a symmetric system with a nonconserved order parameter (spin-flip dynamics), and in Ref. 4 we extended the analysis to the case of a conserved order parameter (spinodal decomposition). In both cases we showed how the dominant length, $L(t)$, develops naturally out of the theory, and we were led to a qualitative understanding of many of the known phenomena for such systems: domain growth and the related development of a Bragg peak, scaling phenomena associated with the peak, and the equilibration of local degrees of freedom. The approach developed allowed for detailed treatment of these various phenomena as functions of the temperature, T_I, before a rapid quench, the final temperature, T_F, after the quench, and the time after the quench.

The structure of the theory developed in MV and also in Ref. 5 was based on a perturbation-theory analysis which is extremely difficult to implement at higher orders and appears highly technical. It is therefore natural to question the generality and the convergence of the method. In Ref. 4 we indicated that the theory developed in MV could be reformulated in a more physical and flexible form and discussed the general structure of the theory only qualitatively. In this paper we return to the case of a nonconserved order parameter and show how the theory, of the type discussed in Ref. 4, can be reformulated in a systematic[6] fashion. From the resulting recursion relations we find new analytical results which elucidate the role of temperature in the scaling behavior of these systems. We also present new results for correlations in coordinate and Fourier space which are of sufficient quality to allow direct comparison with Monte Carlo simulations. Our results are valid also at times and distances longer than those accessible to computer simulations.

A key ingredient in our theoretical development is the time-scaling factor Δ. In MV we assumed that the Δ used in treating unstable growth is the same as that governing

fluctuations near equilibrium. This assumption is not correct. It leads to the result that $\Delta \to 0$ as $T_F \to 0$, which, in turn, produces the physical long-time "freezes" and logarithmic decay found in MV. In Ref. 4 we mentioned that one must develop a self-consistent method for determining Δ. In Sec. III of this paper we discuss the proper determination of Δ in the nonconserved case. We obtain the result $\Delta = b^{-2}$ (where b is the length-rescaling factor) for all $T_F \leq T_c$. We then easily find the correct long-time curvature-driven Cahn-Allen[7] growth law:

$$L(t) = L_0 t^{1/2} . \tag{1.1}$$

An interesting aspect of our theory, not emphasized previously, is our ability to study correlations in coordinate space as a function of time. We study the correlation of spins at $\vec{R}_i$ and $\vec{R}_j$ as functions of $\vec{R}_i - \vec{R}_j$ and the time after the quench. This will give us additional information about the way in which order spreads through the system. We also reanalyze the quasistatic structure factor taking into account the refinements mentioned above. Our main results include the following:

(i) A discussion of correlation functions in coordinate space for distances $\lesssim 100$ (measured in lattice spacings) and at different angles gives direct information about directional aspects of domain growth.

(ii) Calculations of the nearest-neighbor correlation function $\epsilon(1,0;t)$ indicate that it satisfies a scaling relation,

$$\epsilon(1,0;t) = \epsilon(1,0;\infty) + t^{-x} f_\epsilon(\xi/t^x) \tag{1.2}$$

(for sufficiently long times), where ξ is the equilibrium correlation length corresponding to the final equilibrium state and the exponent $x = \frac{1}{2}$. We give explicit results for $f_\epsilon(x)$.

(iii) We have performed Monte Carlo (MC) simulations for $\epsilon(1,0;t)$ and compared them directly with our RG calculations. For[8] times $t \lesssim 1$ we obtain essentially perfect agreement between the MC results and the RG calculations. For longer times the RG calculations lie systematically above the MC simulations. This is due primarily to finite-size effects in the MC simulations associated with metastable configurations.[9] These configurations have the basic effect that $\epsilon(1,0;\infty)_{\mathrm{MC}}$ does not appear to equal the appropriate equilibrium value $\epsilon(1,0;T_F)$. Taking this into account and comparing $\Delta\epsilon = \epsilon(1,0;t) - \epsilon(1,0;\infty)$, we again obtain very good agreement between the MC and RG results.

(iv) For sufficiently small wave numbers and long times ($t \gtrsim 5$) the structure factor is characterized by a central peak which satisfies the scaling relation

$$\tilde{C}(\vec{q},\xi,t) = C_m F(\vec{q}/q_w, q_w \xi) , \tag{1.3}$$

where C_m is the maximum value of the peak (at $\vec{q} = \vec{0}$) and $q_w(t)$ is the half-width of the peak. These quantities, in turn, satisfy the scaling relations

$$q_w(t,\xi) = t^{-x} f_w(\xi/t^x) , \tag{1.4}$$

$$C_m(t,\xi) = m_E^2 t^{2x} f_m(\xi/t^x) , \tag{1.5}$$

where $x = \frac{1}{2}$ and m_E is the equilibrium spontaneous magnetization for the final state. We give explicit results for f_w, f_m, and F.

(v) The angularly averaged function $F(x,0)$, we find, falls off for large x as x^{-p}, where p is approximately 3.1. This is in good agreement with Perod's law[10] and the results of Ohta, Jasnow, and Kawaski[2] that $p = d+1 = 3$. It is also within the error bars of the Monte Carlo calculations of Sahni *et al.*[9] ($p = 2.9$) and Kaski *et al.*[11] ($p = 2.7$). Our angularly averaged shape function is also in rough agreement with that of Ref. 2 (see Sec. IV) over the entire range of x.

(vi) We find an interesting and nontrivial angular dependence for the shape function for large values of x. This seems to indicate, in keeping with the analysis in coordinate space, that the shape function contains some information about the pattern of domain growth.

(vii) We conclude that the controlled growth calculations of Sahni *et al.*,[12] which show that the rate of decrease in area of patch of down spins in a sea of up spins increases with decreasing temperature, is a local effect which is strongly dependent on the particular details of the growth pattern studied.

(viii) Working directly at the transition temperature ($T_F = T_c$) we find that

$$\epsilon(1,0;t) - \epsilon(1,0;\infty) \sim t^{-5/8} , \tag{1.6}$$

$$q_w \sim t^{-1/2} , \tag{1.7}$$

and

$$C_m \sim t^{7/8} , \tag{1.8}$$

for long times.

II. RECURSIVE METHODS FOR OBSERVABLES

A. General comments

The theory developed in MV was based on RG arguments which required implementation of a complicated perturbation-theory expansion which treated the effective interaction between cells as a small parameter. We believe that the structure of the theory we developed in MV is considerably more general than the analysis used there to establish it. In this section we reformulate our approach in a perturbation-theory-independent fashion. The analysis may appear different from that developed in MV, but the final results are quite similar in structure.

B. Perturbation-theory-independent renormalization

A basic tenet of the RG (Ref. 13) is that after averaging over local degrees of freedom and rescaling lengths by a factor $b > 1$, the new "true" equilibrium correlation length ξ', describing the decay of correlations in the coarse-grained system, is related to the correlation length in the original problem by

$$\xi' = \xi/b . \tag{2.1}$$

Let us carefully investigate the consequences of (2.1). In the case of the ferromagnetic Ising model on a square lattice, in zero field, one can calculate[14] ξ exactly as a function of $K = J/k_B T$ (where J is the exchange coupling and

T is the temperature). It is then straightforward to invert (2.1) to obtain the recursion relation for K,

$$\phi' = \phi^b , \tag{2.2}$$

where

$$\phi = e^{2K}\tanh K \tag{2.3}$$

relates the couplings K and K' on the original and renormalized lattice. The fixed-point properties of (2.2) give the exact results for the transition temperature ($\tanh K_c = \sqrt{2}-1$) and the critical index $\nu = 1$. The recursion relation (2.2) was used extensively in our previous work,[15,16] but its use was justified in a different manner.

C. Thermodynamics

The recursion relation (2.2) for K' will be used to "drive" recursion relations for observables. Consider first the equilibrium magnetization density $m_E(K)$. In our previous work[16] we found that m_E satisfies a recursion relation of the form

$$m_E(K) = \nu(K) m_E(K') , \tag{2.4}$$

where $\nu(K)$ is a smooth function of K. The point of view we take here is that $\nu(K)$ is defined by (2.4) and its usefulness is that it is easier to approximate than $m_E(K)$. In the case of the Ising model on a square lattice, where we know $m_E(K)$ exactly,[17] we can use (2.2) and (2.4) to calculate $\nu(K)$ exactly for $T \le T_c$. The resulting $\nu(K)$ is a smooth function of K varying between 1 (as $K \to \infty$) and $b^{-1/8}$ at T_c. Near the transition (for $b = 2$),

$$\nu = (1/2^{1/8})[1 + (K - K_c)/\sqrt{2} + \cdots] . \tag{2.5}$$

In problems where we do not know m_E exactly, we believe it will be a good strategy, given an approximate solution to (2.1), to construct approximations for $\nu = m_E/m_E'$, which depends only on the ratio of m_E and m_E', and then iterate (2.4) to obtain $m_E(K)$. This same type of strategy will be used below in treating spatial structure and time-dependent effects.

Let us turn now to the susceptibility X. If we generalize our analysis of the magnetization to include a magnetic field,[18] take derivatives with respect to the field, and then set it to zero, we obtain a recursion relation of the form

$$X(K) = X_0(K) + b^d \nu^2(K) X(K') . \tag{2.6}$$

For $T > T_c$, $X_0 = 0$, and we obtain

$$X = b^d \nu^2 X' . \tag{2.7}$$

This is of exactly the same form as we found in Refs. 16 and 19, while (2.6) is of the form used in Ref. 20. Here, however, (2.7) serves to define the quantity ν in the disordered phase. Again ν should be a smooth function of K. Using known[21] exact results for X it is easy to show that ν, derived using (2.7) for $K \le K_c$, reduces to (2.5) for T near T_c. Since (2.5) was originally derived using (2.4) for $K \ge K_c$, ν and its derivative are continuous at T_c. It is not difficult to find a reasonable approximation for ν which ties together the easily available high-temperature–expansion results and the result (2.5) valid near T_c. A simple interpolation for $T \ge T_c$ is

$$\nu^2 = \tfrac{1}{4} + u + 2u^2 + u^3 - 8u^4 + Au^5 + Bu^6 , \tag{2.8}$$

where $u = \tanh K$, $A = -19.279\,696\,310\,4$, and $B = 46.142\,840\,511\,6$. The iterated solution for X, using the ν^2 in (2.7), gives excellent results for all $u < u_c$.

In the ordered phase one must allow[20] for a nonzero value of X_0. For low temperatures, where $y = e^{-4K}$ is small, $X \sim 4y^2$, $\nu \to 1$, and, since $K' \sim 2K$, $X' \sim 4y^4$. Therefore, $X = X_0 = 4y^2 + O(y^3)$. A key question is whether X_0 is a smooth function of temperature. If it is divergent then it is as difficult to calculate as X. Since we know so much about X in the two-dimensional (2D) Ising case, we can check this point explicitly. According to Ref. 21 the susceptibility near T_c can be written in the form

$$X = C_{0,\pm} K_c^{7/4} |\delta K|^{-7/4}[1 + r_\pm |\delta K| + O(1)] , \tag{2.9}$$

where $\delta K = K - K_c$, the amplitudes $C_{0,+} = 0.962\,581\,732\,2$ and $C_{0,-} = 0.025\,536\,971\,9$, and $r_\pm = \pm\sqrt{2}/8$. Since we know $\nu(K)$ and $K'(K)$ near T_c, we can compute

$$\begin{aligned} X_0 &= X - 4\nu^2 X' \\ &= C_{0,-} K_c^{7/4} |\delta K|^{-3/4}(r_- + \sqrt{2}/8) + O(1) . \end{aligned} \tag{2.10}$$

We obtain the rather remarkable result that the divergent part of X_0 vanishes only if we use the exact expression for $r_- = -\sqrt{2}/8$. Thus we have the exact result that X_0 is of $O(1)$ at T_c.

Since we have chosen $X_0 = 0$ for $T > T_c$, we require that $X_0 \to 0$ as $T \to T_c$ from below. If we assume that X_0 is of the form

$$X_0 = m_E^2 f , \tag{2.11}$$

then f can be written approximately in the form

$$f = 4y^2 + 32y^3 + 240y^4 + Ay^5 , \tag{2.12}$$

where the first three terms come from a low-temperature expansion and the value of A is adjusted to give the correct amplitude, $C_{0,-} = 0.0255\ldots$, for X. We obtain $A = -1632.4$. A more sophisticated analysis will be given elsewhere. The resulting expression for X agrees with the interpolation form of Ref. 22 to better than 1% for all $T \le T_c$.

The key point in our treatment of thermodynamics is that the multiplicative (ν) and inhomogeneous parts (X_0) of recursion relations (2.4) and (2.6) are smooth functions whose behavior in certain limits is well known, and are, therefore, easy to approximate.

D. Spatial structure

It is very useful, in studying the growth of order, to be able to treat spatial correlations. This requires that we be able to treat the equilibrium correlation functions:

$$\epsilon(\vec{m}) = \langle \sigma_{\vec{m}} \sigma_{\vec{0}} \rangle , \tag{2.13}$$

where $\vec{m} = m_x \hat{x} + m_y \hat{y}$ m_x with m_x and m_y integers, $\sigma_{\vec{m}}$ is an Ising spin at lattice site $\vec{m}$ (we have set the lattice

constant equal to 1), and $\langle\ \rangle$ indicates an equilibrium average depending on the coupling K. We must also be able to accurately calculate the static structure factor

$$\tilde{C}(\vec{q})=\sum_{\vec{m}} e^{+i\vec{q}\cdot\vec{m}}[\epsilon(\vec{m})-m_E^2] \tag{2.14}$$

over a broad range of values of $\vec{q}$ and K.

A very useful aspect of our previous[16,19] RG development was our ability to compute equilibrium short-range correlation functions such as $\epsilon(\vec{m})$ conveniently and to high accuracy. The arguments in those papers explaining the reasons for this accuracy were obscured by rather formal considerations. Let us here, therefore, approach the problem using the ideas developed in the preceding section.

Since the susceptibility is, to within trivial factors, the $\vec{q}=\vec{0}$ component of $\tilde{C}(\vec{q})$, it seems natural to assume that $\tilde{C}(\vec{q})$ satisfies a recursion relation which is a straightforward generalization of (2.6):

$$\tilde{C}(\vec{q},K)=C_0(\vec{q},K)+P(\vec{q},K)\tilde{C}(b\vec{q},K') , \tag{2.15}$$

where we have included the explicit dependence on the coupling and taken into account that we must rescale wave numbers by a factor b on the coarse-grained lattice. Comparing (2.15) and (2.6), we find immediately that

$$C_0(\vec{0},K)=X_0 , \tag{2.16}$$

$$P_0(\vec{0},K)=b^d\nu^2 . \tag{2.17}$$

All of our previous RG work has led to recursion relations for $\tilde{C}(\vec{q})$ of this form.

We assume that C_0 and P are well behaved and local, and, therefore, easy to approximate. Indeed, we have already shown that the long-wavelength components of $C_0(\vec{q})$ and $P(\vec{q})$ are well-behaved functions of temperature.

There are restrictions on the function $P(\vec{q})$. It is unphysical for large-wave-number components of $\tilde{C}(\vec{q},K)$ (except reciprocal-lattice vectors) to be mapped onto X under iteration of the recursion relation. Otherwise they would diverge with X at T_c. Such a mapping arises for wave numbers $\vec{q}_b=2\pi\vec{m}/b$ (and $\vec{q}_b$ is not a reciprocal-lattice vector). We prevent this by demanding that

$$P(\vec{q}_b)=0 . \tag{2.18}$$

For $b=2$ this requires that $P(\vec{q})$ vanish at the edge of the Brillouin zone. Consequently, we call this the "edge condition."

It will be convenient to introduce the Fourier transforms

$$C_0(\vec{q})=\sum_{\vec{m}} e^{i\vec{q}\cdot\vec{m}}\epsilon_0(\vec{m}) , \tag{2.19}$$

$$P(\vec{q})=\sum_{\vec{m}} e^{i\vec{q}\cdot\vec{m}}\Pi(\vec{m}) . \tag{2.20}$$

Taking the Fourier transform of (2.15), we see first that the uniform parts arising from the m_E^2 and $(m_E')^2$ subtractions in (2.14) cancel because of (2.4) and the result.

$$\sum_{\vec{n}}\Pi(\vec{m}-b\vec{n})=\sum_{\vec{n}}\int\frac{d^dq}{(2\pi)^d}e^{+i\vec{q}\cdot(\vec{m}-b\vec{n})}P(\vec{q})$$
$$=b^{-d}P(\vec{0})=\nu^2 . \tag{2.21}$$

It follows that

$$\epsilon(\vec{m})=\epsilon_0(\vec{m})+\sum_{\vec{n}}\Pi(\vec{m}-b\vec{n})\epsilon'(\vec{n}) . \tag{2.22}$$

The fixed-length sum rule for Ising spins $(\sigma_{\vec{m}})^2=1$ gives a strong constraint on this recursion relation. Since $\epsilon(\vec{0})=\epsilon'(\vec{0})=1$, we have

$$1=\epsilon_0(\vec{0})+\sum_{\vec{n}}\Pi(-b\vec{n})\epsilon'(\vec{n}) . \tag{2.23}$$

Since the left-hand side of (2.23) is independent of temperature, we choose $\Pi(\vec{m})$ such that the right-hand side is independent of all $\epsilon(\vec{n})$ except $\epsilon'(\vec{n}=\vec{0})$. This requires that

$$\Pi(\vec{m})=0 \tag{2.24}$$

for $|m_x|,|m_y|\geq b$. Somewhat weaker constraints are possible, but they seem physically (and practically) less attractive. In the case $b=2$ we have that $\Pi(\vec{m})$ is restricted to the three independent components $\Pi(\vec{0})$, $\Pi(0,1)$, and $\Pi(1,1)$. The Fourier transform is given by

$$P(\vec{q})=\Pi(\vec{0})+4\Pi(1,0)g_1(\vec{q})+4\Pi(1,1)g_2(\vec{q}) , \tag{2.25}$$

where

$$g_1(\vec{q})=\tfrac{1}{2}(\cos q_x+\cos q_y) , \tag{2.26a}$$

$$g_2(\vec{q})=\cos q_x\cos q_y . \tag{2.26b}$$

The edge conditions (2.18), (2.17), and (2.24) are sufficient to determine the three $\Pi(\vec{m})$ in (2.25). We obtain

$$\nu^2=\Pi(\vec{0})=4\Pi(1,1)=2\Pi(1,0) \tag{2.27}$$

and

$$P(\vec{q})=\nu^2 f(\vec{q}) , \tag{2.28}$$

with

$$f(\vec{q})=1+2g_1(\vec{q})=g_2(\vec{q}) . \tag{2.29}$$

$P(\vec{q})$ is of precisely the same form as we found in our previous work. Clearly, this analysis can be generalized to other b and d values.

We are now left with the determination of $C_0(\vec{q})$, or, equivalently, the $\epsilon_0(\vec{m})$. The basic assumption here is that the $\epsilon_0(\vec{m})$ fall off rapidly with increasing $|\vec{m}|$, and approximations where $\epsilon_0(\vec{m})=0$ for all $|\vec{m}|>m_0$ should give good results for rather small values of m_0. For a given choice of m_0, we can determine the $\epsilon_0(\vec{m})$, for $|\vec{m}|\leq m_0$, using (2.22), if we know $\epsilon(\vec{m})$ and $\epsilon'(\vec{m})$ for $|\vec{m}|<m_0$. This is not difficult in practice since the $\epsilon(m)$'s, for small $|\vec{m}|$, are the easiest quantities to approximate using series, Monte Carlo, etc.

We must modify this program only slightly if we are to satisfy (2.16). This condition can simply replace the re-

cursion relation for $\epsilon(\vec{m})$ for $|\vec{m}|$ nearest to m_0. In this paper we shall be satisfied with the lowest-order nontrivial approximation corresponding to $m_0=\sqrt{2}$. We shall investigate the convergence of this series of approximation elsewhere. The "model" $m_0=\sqrt{2}$ corresponds to writing

$$C_0(\vec{q})=\epsilon_0(\vec{0})+4\epsilon_0(1,0)g_1(\vec{q})+4\epsilon_0(1,1)g_2(\vec{q}) , \tag{2.30}$$

and the three independent components are determined by (2.23), which gives

$$1=\epsilon_0(\vec{0})+\Pi(\vec{0}) , \tag{2.31}$$

(2.16), and (2.22) with $\vec{m}=(1,0)$. It is easy to solve this set of equations to obtain

$$\epsilon_0(\vec{0})=1-\nu^2 , \tag{2.32a}$$

$$\epsilon_0(1,0)=\epsilon(1,0)-\nu^2[1+\epsilon'(1,0)]/2 , \tag{2.32b}$$

$$\epsilon_0(1,1)=\tfrac{1}{4}(X_0+\nu^2-1-4\{\epsilon(1,0)-\nu^2/2[1+\epsilon'(1,0)]\}) . \tag{2.32c}$$

Since $\epsilon(1,0)$ is known exactly[23] for the 2D Ising model, we can compute the $\epsilon_0(\vec{m})$ explicitly. They are smooth functions of K which do not warrant further discussion here. If we introduce the quantities

$$r=2\epsilon_0(1,0)+\nu^2 \tag{2.33a}$$

and

$$s=4\epsilon_0(1,1)+\nu^2 , \tag{2.33b}$$

then

$$C_0(\vec{q})=1+2rg_1(\vec{q})+sg_2(\vec{q})-P(\vec{q}) . \tag{2.34}$$

Taking this equation with (2.26) we see that (2.15) is of the same form as that obtained in Refs. 16 and 19 if r and s are associated with the nearest- and next-nearest-neighbor correlation functions in a "cell." In the development here we have not needed to break up the system into cells and it should be apparent how we could improve the approximation.

The iterated solution of the recursion relation for $\tilde{C}(\vec{q})$ leads to very good results for $\tilde{C}(\vec{q})$ over a wide range of $\vec{q}$ and K. Since approximations similar to that derived here have been discussed extensively elsewhere,[3,15,16,19] and have led to good results, we will not discuss this further here.

E. Nonequilibrium behavior.

We move to the nonequilibrium case where we have a sudden temperature quench from coupling $K_I<K_c$ to $K_F>K_c$. We assume that the nonequilibrium probability distribution is given in this case for times t after the quench by

$$P[\sigma,t]=e^{D_\sigma(K_F)t}P[\sigma,K_I] , \tag{2.35}$$

where $P[\sigma,K_I]$ is the initial equilibrium probability distribution and $D_\sigma(K_F)$ is a spin-flip operator characterized by a basic flipping rate α (we typically set $\alpha=1$ below) and a flipping probability[24] for the spin at site i,

$$W_i[\sigma]=\tfrac{1}{2}\left[1-\frac{a_F}{2}\sigma_i\sigma_i^T+\frac{a_F^2}{4}\sigma_i^P\right] , \tag{2.36}$$

where $a_F=\tanh 2K_F$, σ_i^T is the sum of the four nearest neighbors of the spin at site i, and σ_i^P is the sum of the products of next-nearest neighbors formed by the nearest neighbors of σ_i. The quasistatic structure factor is given by

$$\tilde{C}(\vec{q},t)=\sum_\sigma P[\sigma,t]\sum_{\vec{m}} e^{+i\vec{q}\cdot\vec{m}}\sigma_{\vec{m}}\sigma_{\vec{0}} . \tag{2.37}$$

We assume here that the generalization of the static recursion relation (2.15) to the nonequilibrium regime takes the form

$$\tilde{C}(\vec{q},t)=C_0(\vec{q},t)+P(\vec{q},t)\tilde{C}(b\vec{q},\Delta t) . \tag{2.38}$$

An important new quantity in this equation is the time-rescaling factor Δ. We will discuss Δ in some detail later; for now we note that it is in the range of $0\le\Delta\le 1$.

The arguments we gave in the static case which led to the "edge condition" (2.18) are still applicable in the dynamic case as is the sum rule

$$\int\frac{d^dq}{(2\pi)^d}\tilde{C}(\vec{q},t)=\sum_\sigma P[\sigma,t]=1 . \tag{2.39}$$

Hence we can reduce $P(\vec{q},t)$ to the form

$$P(\vec{q},t)=\nu^2(t)f(\vec{q}) , \tag{2.40}$$

where $f(\vec{q})$ is given by (2.29), and we require

$$\nu^2(0)=\nu^2(K_I) , \tag{2.41a}$$

$$\nu^2(\infty)=\nu^2(K_F) . \tag{2.41b}$$

Similarly, it is straightforward and natural to assume that in a lowest-order approximation, $C_0(\vec{q},t)$ is of the same form as $C_0(\vec{q})$ in (2.30), but with the $\epsilon_0(\vec{m})$ replaced by $\epsilon_0(\vec{m},t)$. Again, since the $\epsilon_0(\vec{m},t)$ are expected to be local in time and space, we assume that they evolve in time rather rapidly from their initial values $\epsilon_0(\vec{m},K_I)$ to their final equilibrium values $\epsilon_0(\vec{m},K_F)$.

In this paper we will take a simple and direct approach to the quantities $\nu^2(t)$ and $\epsilon_0(\vec{m},t)$. More sophisticated schemes will be discussed elsewhere. Here we develop only the simplest approximations for the quantities $\nu^2(t)$ $\epsilon_0(\vec{0};t)$, $\epsilon_0(1,0;t)$, and $\epsilon_0(1,1;t)$. These approximations, however, lead to quite good results, as we shall see.

We first note that the sum-rule condition (2.39) requires that

$$1=\epsilon_0(\vec{0};t)+\nu^2(t) \tag{2.42}$$

for all times. We have, therefore, only three independent quantities which, we argue, equilibrate on a short-time scale. It therefore seems reasonable to fix this time scale in terms of the initial response of the system after the quench. We find easily, from the Fourier transform of (2.37), that

$$\frac{\partial}{\partial t}\epsilon(\vec{m};t)\bigg|_{t=0}=\langle\tilde{D}_\sigma(\sigma_{\vec{m}}\sigma_{\vec{0}})\rangle_{t=0} , \tag{2.43}$$

where the average is over the initial state and $\tilde{D}_\sigma$ is the adjoint of D_σ (see Refs. 16 and 25). If, as we assume in the rest of this paper, the initial state is completely disordered ($K_I=0$), then we obtain the very simple result

$$\frac{\partial}{\partial t}\epsilon(\vec{m};t)\bigg|_{t=0}=a_F\sum_a \delta_{\vec{m},\vec{\delta}_a}\ , \tag{2.44}$$

where $\vec{\delta}_a$ is a vector connecting nearest neighbors. The corresponding result for the structure factor is

$$\frac{\partial}{\partial t}\tilde{C}(\vec{q},t)\bigg|_{t=0}=4a_F g_1(\vec{q})\ , \tag{2.45}$$

where $g_1(\vec{q})$ is given by (2.26a). In view of the above arguments, it seems appropriate to use

$$\frac{\partial}{\partial t}\epsilon(1,0;t)\bigg|_{t=0}=a_F \tag{2.46}$$

and

$$\frac{\partial}{\partial t}\tilde{C}(\vec{0},t)\bigg|_{t=0}=4a_F \tag{2.47}$$

to tie down the time scales associated with the $\epsilon_0(\vec{m};t)$ and $\nu^2(t)$. Before doing so, however, we should interject some physical information. In recursion relations of the type given by (2.38), one wants the long-distance behavior to be carried by the rescaled variable. Alternatively, one wants the inhomogeneous term like $X_0=0$ to be as small as possible. Indeed, in the disordered phase we have $X_0=0$. Similarly, one wants to include the bulk of the long-wavelength dependence of $\tilde{C}(\vec{q},t)$ in the coarse-grained term. It therefore makes sense to require

$$\frac{\partial}{\partial t}C_0(\vec{0},t)\bigg|_{t=0}=0\ . \tag{2.48}$$

We assume that $\nu^2(t)$ and $\epsilon(1,0;t)$ have relaxational forms:

$$\nu^2(t)=\nu_F^2+e^{-\lambda t}(\nu_I^2-\nu_F^2)\ , \tag{2.49}$$

$$\epsilon_0(1,0;t)=\epsilon_0(1,0;K_F)+e^{-\lambda_1 t}[\epsilon_0(1,0;K_I)-\epsilon_0(1,0;K_F)]\ , \tag{2.50}$$

and the rates λ and λ_1 are to be determined. We allow for the possibility that λ and λ_1 may be somewhat different. We expect $\epsilon_0(1,1;t)$, however, to relax with a rate similar to $\epsilon_0(1,0;t)$, but with a rather different initial slope. We therefore assume a form

$$\epsilon_0(1,1;t)=\epsilon_0(1,1;K_F)+e^{-\lambda_1 t}[\epsilon_0(1,1;K_I)-\epsilon_0(1,1;K_F)+At]\ , \tag{2.51}$$

with A to be determined. It is straightforward, using the recursion relations for $(\partial\tilde{C}(\vec{0},t)/\partial t)_0$ and $(\partial\epsilon(1,0;t)/\partial t)_0$ and (2.48) to solve, using the exact results (2.46) and (2.47), for λ, λ_1, and A:

$$\lambda=4(a_F-\Delta a_F')/(4\nu_F^2-1)\ , \tag{2.52}$$

$$\lambda_1=(4a_F+3\,\Delta a_F')/[1+4(r_F^2-\nu_F^2)]\ , \tag{2.53}$$

and

$$A=\tfrac{1}{4}[-\lambda_1 X_0(K_F)+(\lambda-\lambda_1)(\nu_F^2-\nu_I^2)]\ . \tag{2.54}$$

This then ties down all of the ingredients in our recursion relation (2.38) except Δ, which we discuss in the next section.

III. DETERMINATION OF Δ AND SCALING RELATIONS

The time-rescaling factor Δ plays a very important role in our analysis, and as we shall see, controls the basic growth laws operating in the system. The determination of Δ is therefore an important aspect of our theory.

Clearly, the role of Δ is associated with the idea of self-similarity developed in Sec. III of MV. We argued there that on a long-time and -distance scale the quasistatic structure factor should show self-similarity under rescaling of space and time. In this limit, where $\tilde{C}(\vec{q},t)$ is sharply peaked near $\vec{q}=\vec{0}$, the C_0 term can be safely neglected in recursion relation (2.38), which then reduces to

$$\tilde{C}(\vec{q},t,\xi)=b^d\nu_F^2\tilde{C}(b\vec{q},\Delta t,\xi/b)\ , \tag{3.1}$$

where ν_F is defined by (2.4) and we have written the arguments of $\tilde{C}$ explicitly. (See the discussion at the beginning of Sec. V A in MV.) The Fourier transform of (3.1) gives, in coordinate space,

$$\tilde{C}(\vec{r},t,\xi)=\nu_F^2 C(\vec{r}/b,\Delta t,\xi/b)\ . \tag{3.2}$$

Let us define the quantity

$$R_L(t,\xi)=L^{-2d}\int_0^L d^d r\, d^d r'\tilde{C}(\vec{r}-\vec{r}',t,\xi)\ . \tag{3.3}$$

Equation (3.2) then leads to the result

$$R_L(t,\xi)=\nu_F^2 R_{L/b}(\Delta t,\xi/b)\ . \tag{3.4}$$

Note that if the quench is to zero temperature, then $\xi=\xi'=0$ and $\nu_F=1$, and we have the relation

$$R_L(t)=R_{L/b}(\Delta t)\ . \tag{3.5}$$

As a check of this result we carried out a Monte Carlo analysis of $R_L(t)$ for different choices of L, in systems of size $M\times M$ with $M\le 16$ and $L\le M/2$. Self-similarity implies that, by rescaling time by Δ, the plots of R_L versus time, for various L, should all coincide. We see in Fig. 1 that this is indeed the case. In that figure we have taken $\Delta=b^{-2}$ (as we will establish in detail below). Thus our self-similarity assumption seems well founded.

We shall examine several methods for determining Δ which all lead to the same result. The first method, though somewhat heuristic, is physically appealing and in the spirit of the Cahn-Allen[7] analysis.

If we take the derivative of (3.1) with respect to time and then divide by (3.1), we obtain

$$\Delta=\lim_{t\to\infty}\lim_{q\to 0}\frac{(d/dt)\ln\tilde{C}(\vec{q},t,0)}{(d/dt)\ln\tilde{C}(\vec{q}\,',t',0)}\ . \tag{3.6}$$

Since

$$\frac{\partial}{\partial t}\tilde{C}(\vec{q},t,0)=\frac{1}{N^2}\sum_{\vec{n},\vec{m}}e^{i\vec{q}\cdot(\vec{m}-\vec{n})}\langle\tilde{D}_\sigma\sigma_{\vec{m}}\sigma_{\vec{n}}\rangle_t\ , \tag{3.7}$$

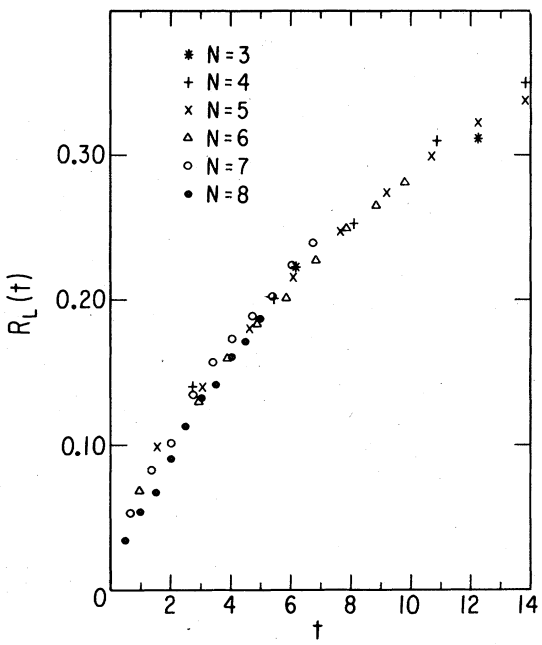

FIG. 1. Scaled quantity R_L, defined by (3.3), vs time for various choices of $L=N-1$ for a quench from $u_I=0$ to $u_F=1$. The solid circles correspond to $R_L(t)$ for an 8×8 system with a length of seven lattice spacings. The other data correspond to smaller systems with their times rescaled by a factor $\Delta^{-1}=b^{+2}$, where b is the ratio of the values of L_N to $L_8=7$.

we realize that as $t\to\infty$, the system equilibrates, and $\langle \tilde{D}_\sigma \sigma_i \sigma_j \rangle_t \to 0$. At zero temperature the equilibrium state is the completely ordered state. Furthermore one can also easily see that a perfectly uniform wall between up and down regions is also stable at zero temperature. The last step in the production of smooth walls which produces a nonzero contribution to $\partial\tilde{C}(\vec{q},t,0)/\partial t$, is the annihilation of a kink on an otherwise smooth wall. It is straightforward to show that such a process produces a contribution to $\partial\tilde{C}(\vec{q},t,0)/\partial t$ proportional to $q^2\tilde{C}(\vec{q},t,0)$. It follows, then, from (3.6), that

$$\Delta(T_F=0)=b^{-2} . \tag{3.8}$$

In a similar fashion, if one replaces σ_i by a scalar field $\phi(\vec{r})$, and $\tilde{D}_\sigma$ with the Fokker-Planck operator associated with the time-dependent Ginzburg-Landau model (model A),[26] and looks for planar solutions of the form $\phi=f[z-z_0(\vec{r}_\perp)]$, where $f(z)$ is the kinklike solution with an interface at $z=z_0(\vec{r}_\perp)$, $z\cdot\vec{r}_\perp=0$, then again one easily finds that $\partial \ln\tilde{C}(\vec{q},t)/\partial t\sim q^2$ and $\Delta=b^{-2}$. This result is independent of temperature for $T<T_c$.

The result that Δ is independent of temperature for $T_F\le T_c$ makes sense if one believes that for sufficiently long times, when domains are very large, temperature fluctuations play no important role.

In developing a more quantitative method for determining Δ, it is useful to investigate some very important consequences of (3.1). Note first that (3.1) has a scaling solution

$$\tilde{C}(\vec{q},t,\xi)=C_m F(\vec{q}/q_w, q_w\xi) , \tag{3.9}$$

where

$$q_w(\Delta t,\xi/b)=b q_w(t,\xi) , \tag{3.10}$$

$$C_m(t,\xi)=b^d v_F^2 C_m(\Delta t,\xi/b) . \tag{3.11}$$

With the assumption that Δ is independent of temperature for $T\le T_c$, (3.10) and (3.11) possess the scaling solutions [using (2.4)]

$$q_w(t,\xi)=t^{-x} f_w(\xi/t^x) , \tag{3.12}$$

$$C_m(t,\xi)=m_E^2 t^y f_m(\xi/t^x) , \tag{3.13}$$

where

$$b\Delta^x=1 , \tag{3.14}$$

$$y=xd . \tag{3.15}$$

These scaling results for q_w and C_m are new and we will explore their consequences in detail in Sec. IV B; here, however, they are useful because they tell us that we can also determine Δ through an analysis of $C_m(t,\xi)$. If we work at $T_F=0$, then $m_E^2=1$, $\xi=0$, and

$$C_m(t)=f_m(0)t^y , \tag{3.16}$$

and by determining y we obtain $\Delta=b^{-(d/y)}$. $C_m(t)$ can be conveniently studied using Monte Carlo methods. For an $N\times N$ system of Ising spins, $C_m(t)$ is related to the average of the total magnetization squared by

$$C_m(t)=\langle M^2\rangle_t/N^2 . \tag{3.17}$$

From a practical point of view, N is fixed at some finite value, and for sufficiently long times, $C_m(t)$ begins to saturate (since its maximum is N^2). Therefore a simulation should not be carried out to very long times. We have carried out a series of simulations for quenches from infinite to zero temperature for various values of N. For fixed N one expects $C_m(t)$ to show a power-law growth with time until finite-size effects become important and it turns over and begins to saturate at its maximum value of N^2. For $N=4$ this "bending" occurs for $t\sim 2$. As N increases these saturation effects are pushed out to longer times. For $N=10$ there is no discernible bending of $C_m(t)$ for times up to $t=5$. This is consistent with the result $C_m(5)=20<10^2$ for $N=10$. Thus we seem to be safe from finite-size effects if we stop at times of 5 or less for N greater than 10.

An important and neglected aspect of this problem is the dependence of Monte Carlo calculations on the number of runs carried out. In the case of equilibrium calculations one expects that calculations can be carried out in roughly two ways. One can carry out n runs on systems of size N^d, or alternatively carry out fewer runs (n/a) on larger systems of size aN^d, and one should obtain similar results. In the nonequilibrium case these standard arguments do not seem to hold. Such effects have been recently discussed by Sadiq and Binder.[27] We have looked at the values of $C_m(t)$ for several times as a function of number of runs averaged over. We have done this, for example, for $N=10$ and 16, and see that the data for the larger system are no better behaved as a function of the number of runs than for the smaller system. These ef-

fects, which have been largely ignored in most Monte Carlo work, are associated with the sensitivity to initial conditions in these nonequilibrium situations. In particular, there are certain metastable configurations[10] which are generated for a particular N which equilibrate very slowly (if at all). Other initial states equilibrate very quickly. One needs a sufficient number of runs to sample all of these various initial states. Of course, such effects will become smaller as one goes to very large systems where one can have local manifestations of each type of initial condition. This appears, however, to require extremely large systems.

With the above thoughts in mind we have carried out many runs (388) for a 16×16 system over the time region from 0 to 5. We obtain a very good fit to the power-law behavior,

$$C_m(t)=0.97+3.62t^{1.02}\ . \tag{3.18}$$

Note that $C_m(0)=1$ exactly, and the 0.97 is a measure of the statistical error in the MC simulation. Clearly, this is consistent with the Cahn-Allen[7] result $2x=y=1$. As a further check on our analysis we have computed x at a much higher temperature ($u_F=0.42$) and find $2x=0.988$ for $N=16$ and a fit to the time region $0<t<5$ over 76 runs. This is clearly consistent with our assessment that x and Δ are temperature independent. We also have carried out this procedure for a three-dimensional, 1000-spin system, and, after 80 runs, obtained $y=1.45$, again in agreement with the result $y=d/2$ for $x=\frac{1}{2}$.

We see that our heuristic arguments are in good agreement with numerical simulations and we can conclude that $\Delta=b^{-2}$ for $T\leq T_c$.

IV. RESULTS

In this section we analyze the numerical solutions of the recursion relations derived in Sec. II. All results presented here are for quenches from infinite temperature ($u_I=0$) to temperatures below T_c ($u_F>u_c=\sqrt{2}-1$). We expect the influence of u_I to be less important and we postpone that part of the analysis to future work.

A. Spatial correlations

We first consider correlations directly in coordinate space. With the rescaling factor $b=2$ it is particularly simple to write recursion relations for spatial correlation functions of the form $\epsilon(2^{N_1},0;t)$ or $\epsilon(2^{N_1},2^{N_2};t)$, where N_1 and N_2 are integers. Since the very-long-range behavior is best studied by considering $\tilde{C}(\vec{q},t)$ at small $\vec{q}$ (as in the next subsection), we will examine here the results at short and intermediate distance ($\lesssim 100$ lattice spacings).

Of primary importance is the nearest-neighbor correlation function $\epsilon(1,0;t)$, the "short-range-order parameter," which satisfies the recursion relation

$$\epsilon(1,0;t)=\frac{r(t)}{2}+\frac{v^2(t)}{2}\epsilon'(1,0;t')\ , \tag{4.1}$$

where [see (2.33a)]

$$r(t)=2\epsilon_0(1,0;t)+v^2(t)\ . \tag{4.2}$$

It follows from the discussion in Sec. II that as $t\to0$ and $t\to\infty$, $\epsilon(1,0;t)$ reduces to the corresponding exact equilibrium values.

The behavior of $\epsilon(1,0;t)$ as a function of time is illustrated in Fig. 2 for several values of u_F. Analysis of the quantity $\epsilon(1,0;t)/\epsilon(1,0;\infty)$ shows only a weak dependence on u_F. This dependence, however, is not quite monotonic with temperature, showing a minimum of $u_F=0.55$ for times of order unity. The time evolution of $\epsilon(1,0;t)$ breaks down into two basic regimes. There is an initial growth period where local equilibrium is established and when the slope is given exactly by (2.46). For longer times there is a crossover to an asymptotic scaling region where

$$\epsilon(1,0;t)-\epsilon(1,0;\infty)=m_E^2t^{-1/2}f_\epsilon(\xi/\sqrt{t})\ . \tag{4.3}$$

The derivation of this result follows directly from (4.1) if we go to times where $r(t)$ and $v^2(t)$ are well approximated by their final values. Then $\Delta\epsilon\equiv\epsilon(1,0;t)-\epsilon(1,0;\infty)$ satisfies the recursion relation

$$\Delta\epsilon(\xi,t)=\frac{v_F^2}{2}\Delta\epsilon(\xi',t')\ . \tag{4.4}$$

Using (2.4), one is led immediately to (4.3). The direct numerical solution of (4.1) gives $f_\epsilon(x)$ as shown in Fig. 3. In the limit $t\to\infty$, for fixed finite correlation length, $f_\epsilon(0)=-0.355$. $f_\epsilon(x)$ increases rather rapidly with x for small x and then grows as $x^{2\beta/\nu}=x^{1/4}$ for large x. At the critical point,

$$\lim_{x\to\infty}[x^{-1/4}f_\epsilon(x)]=-0.536 \tag{4.5}$$

and

$$\Delta\epsilon(t)=-0.407t^{-5/8}\ . \tag{4.6}$$

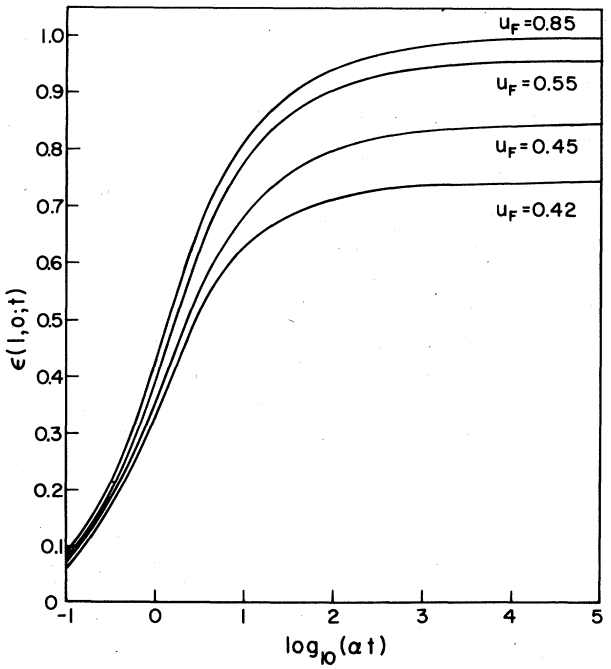

FIG. 2. Nearest-neighbor correlation function [$\epsilon(1,0;t)$] vs time [$\log_{10}(\alpha t)$] for several values of the final temperature.

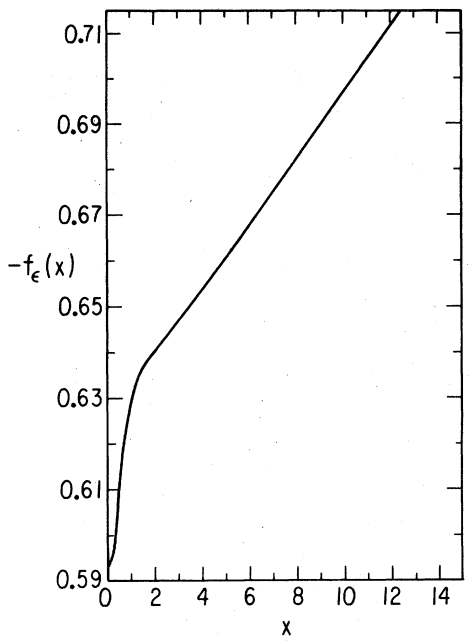

FIG. 3. Shape function $[-f_\epsilon(x)]$ for the nearest-neighbor correlation function, defined by (4.3), vs $x=\xi/\sqrt{t}$.

The system rapidly approaches the scaling regime. For all $u_F \geq u_c$, $\epsilon(1,0;t)$ is given by (4.3) to good accuracy for $t \geq 1.7$.

These results for $\epsilon(1,0;t)$ can be directly compared with Monte Carlo simulations. We have performed such simulations for $u_F=0.6$ on a 16×16 system for times up to 10.6 averaging over 50 runs, and a 90×90 system for times up to 100 averaging over five runs. We find that our RG results (as shown in Fig. 4) agree essentially perfectly with the MC simulations for times $t<1.0$. For longer times they are always somewhat above the MC results, the discrepancy being less than 10% at any time. A primary difference between the MC and RG longer-time results is that $\epsilon(1,0;t)_{\rm MC}$ does not appear to asymptotically approach the equilibrium result $\epsilon(1,0;K_F)$. This effect has been noted by a number of authors[9] and has been attributed to the development of "metastable" configurations which clearly have a disordering effect and reduce $\epsilon(1,0;t)$. If we carry out a linear least-squares fit of the MC data (for the 16×16 system) over the time ranges $3<t<10$ to a form[28]

$$\epsilon(1,0;t)=\epsilon(1,0;\infty)+\epsilon_1/\sqrt{t}\ , \tag{4.7}$$

we obtain $\epsilon(1,0;\infty)=0.932$ and $\epsilon_1=-0.623$. If we carry out precisely the same type of fit for the RG results, we obtain $\epsilon(1,0;\infty)=0.992$ and $\epsilon_1=-0.624$. In this case the exact result is $\epsilon(1,0;K_F)=0.9895\ldots$, and the MC data is not approaching its appropriate final equilibrium value. The excellent agreement between the theory and the MC results for ϵ_1 is very satisfying (although both values have sources of error clearly larger than the difference between them). In Fig. 5 we plot $\Delta\epsilon$ for the theory and the MC simulations, and find excellent agreement.

Let us now consider the longer-range correlations. We have, as stated above, considered correlation functions of the form $\epsilon(2^N,0;t)$ which give information about ordering in the (1,0) direction and satisfy the recursion relation

$$\epsilon(2^{N_1},0;t)=\nu^2(t)\epsilon'(2^{N_1-1},0;t'),\quad N_1\geq1\ . \tag{4.8}$$

We have also considered correlations in the (1,1) direction, $\epsilon(2^{N_1},2^{N_1};t)$, where the relevant recursion relations are

$$\epsilon(1,1;t)=\tfrac{1}{4}[s(t)+2\nu^2(t)\epsilon'(1,0;t)+\nu^2(t)\epsilon'(1,1;t)]\ , \tag{4.9}$$

where

$$s(t)=4\epsilon_0(1,1;t)+\nu^2(t)$$

and

$$\epsilon(2^{N_1},2^{N_1};t)=\nu^2(t)\epsilon'(2^{N_1-1},2^{N_1-1};t) \tag{4.10}$$

for $N_1\geq1$. Finally, to examine directions between (1,0) and (1,1) we have considered $\epsilon(2^{N_1},2^{N_2};t)$, for which

$$\epsilon(2^{N_1},2^{N_2};t)=\nu^2(t)\epsilon'(2^{N_1-1},2^{N_2-1};t)\ , \tag{4.11}$$

with $N_1>N_2\geq1$, and

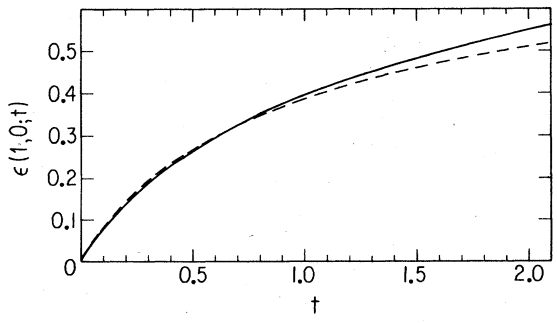

FIG. 4. Nearest-neighbor correlation function $[\epsilon(1,0;t)]$ vs time t for $u_I=0$ and $u_F=0.60$. The solid lines are the results of the RG calculation. The dashed line is the result of a Monte Carlo simulation for a 90×90 system averaged over four runs. Essentially identical MC results were obtained using a 16×16 system averaged over 50 runs.

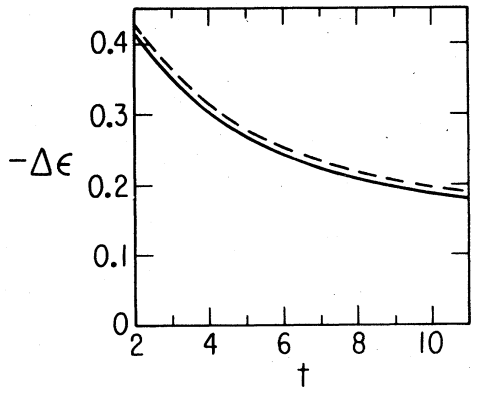

FIG. 5. $-\Delta\epsilon[=\epsilon(1,0;\infty)-\epsilon(1,0;t)]$ vs time t. As in Fig. 4 the solid lines are the RG results and the dashed lines the MC results; $u_F=0.60$.

$$\epsilon(2^{N_1},1;t)=\frac{\nu^2(t)}{2}[\epsilon'(2^{N_1-1},1;t)+\epsilon(2^{N_1-1},1;t)] . \quad (4.12)$$

Combining Eqs. (4.8)—(4.12) with (4.1), all the desired correlation functions can be obtained by iteration. We have investigated these spatial correlations for several u_F values and distances less than 100 lattice spacings. The combined results offer a rather vivid picture of the correlation growth in real space, and, therefore, of the average domain growth.

The correlation functions along the x axis are plotted in Fig. 6, as a function of time, for $u_F=0.42$. One can see that, for $N>0$, their behavior is fairly similar. The bunching up of the long-time values for large values of N is due to the fact that the equilibrium values for long distances do not significantly differ from m_E^2. As N increases it takes longer for the correlation functions to reach their equilibrium value. It is convenient to quantify this by defining a time $t_{eq}(r)$ as the time at which correlations over a distance r have reached 99% of their final equilibrium. At time $t_{eq}(r)$ equilibrium has been achieved over distance of order r, and by studying the relationship between t and r we can gain quantitative information on domain growth. In general, we find that $t_{eq}(r)$ obeys the law

$$t_{eq}(r)=ar^2 . \quad (4.13)$$

This is in agreement with the result $L(t)\sim t^{1/2}$. A fit of t_{eq} to the form ar^z, for correlations in the (1,0) direction give $z=2.03$ and $a=1.5\times10^3$. The data in Fig. 6 is replotted in Fig. 7 as a function of distance (note that $N_1\equiv\log_2 r$) at different times. The dots are the results (at integer N_1) and the lines are guides to the eye only.

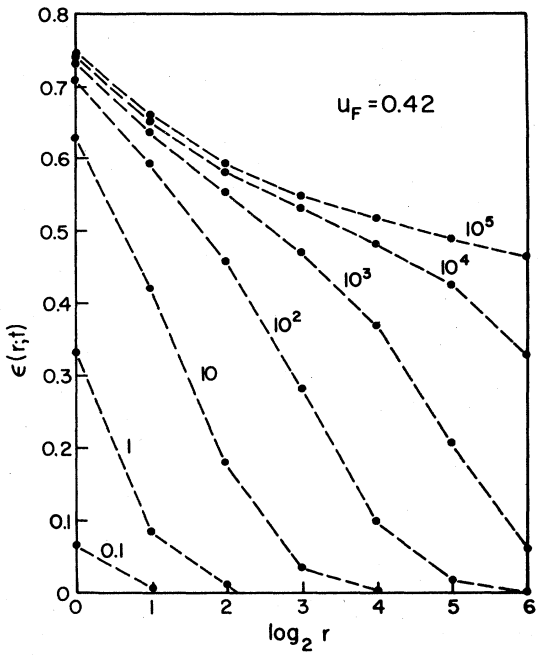

FIG. 7. Spatial correlation functions $[\epsilon(r;t)]$ vs distance $(\log_2 r)$ along the x axis. The dots represent the calculated values, from the recursion relation. The dashed lines are guides to the eye, and the numerical labels on the dashed lines are the values of αt.

The results for correlations in the (1,1) direction are plotted in Fig. 8. These results are similar to those in Fig. 6 except for the $N_1=0$ case. In this case, $z=2.05$ and $a=2.4\times10^3$. The difference in a in the two cases is an anisotropy growth effect (see Fig. 9): the correlation func-

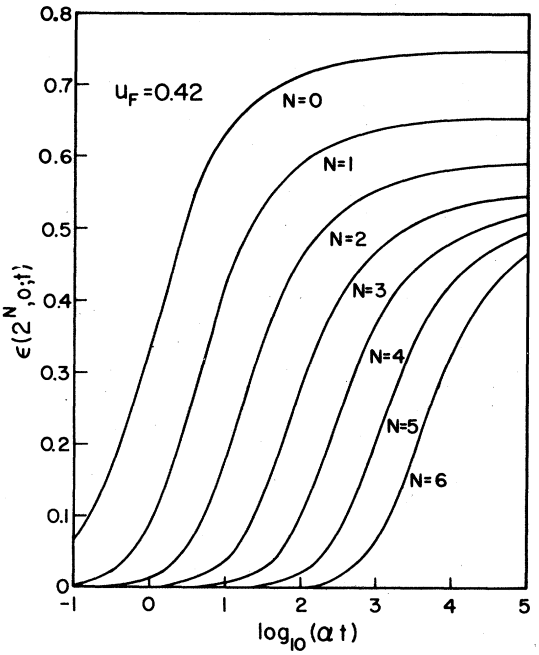

FIG. 6. Spatial correlation functions along the x axis, $[\epsilon(2^N,0;t)]$, vs $[\log_{10}(\alpha t)]$ for values of N from 0 to 6, at $u_F=0.42$.

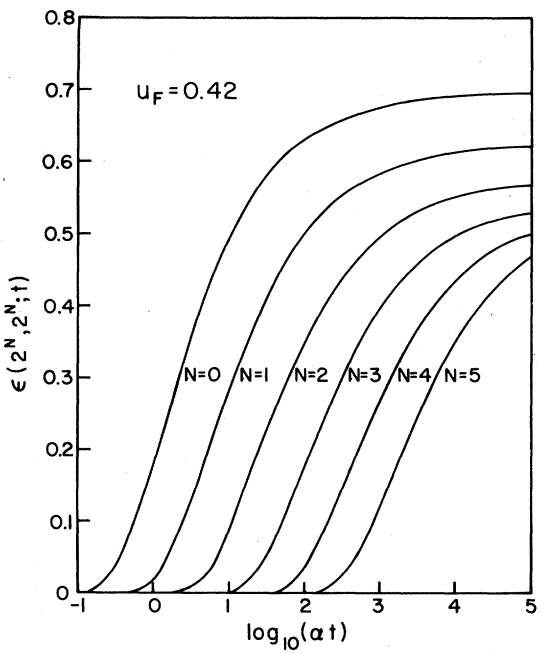

FIG. 8. Spatial correlation functions of the form $\epsilon(2^N,2^N;t)$ [along the (1,1) direction] vs time $[\log_{10}(\alpha t)]$ for $0\leq N\leq 6$ and $u_F=0.42$. This figure should be compared with Fig. 6.

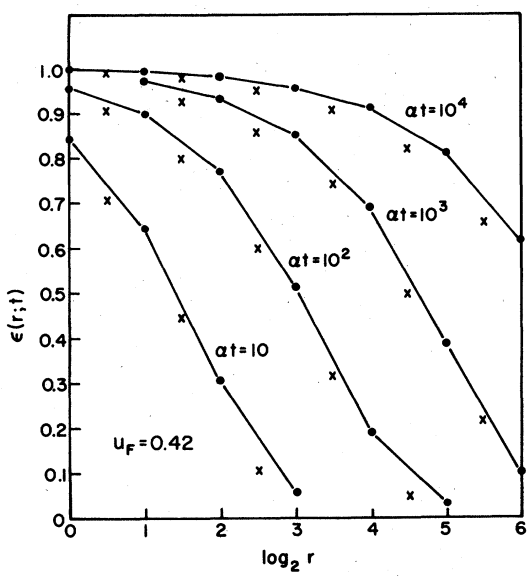

FIG. 9. Spatial correlation functions $[\epsilon(r;t)]$ as a function of distance $(\log_2 r)$ in two different directions: The dots correspond to the x axis and the crosses to the (1,1) direction. The lines joining the dots are for illustrative purposes only, and they are labeled by the time. Note that the crosses appear systematically below what one would expect from interpolation along the x axis. This illustrates the anisotropy discussed in the text.

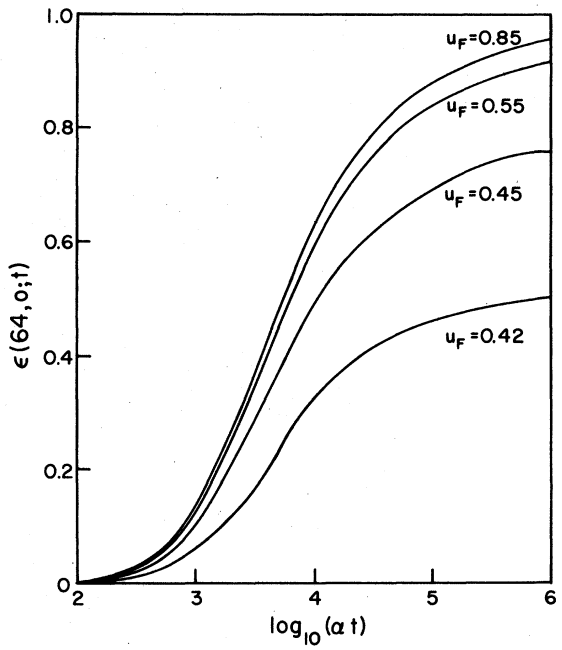

FIG. 10. Correlation function $\epsilon(64,0;t)$ as a function of time $[\log_{10}(\alpha t)]$, for the same values of u_F as in Fig. 2. Note that the different time scale in this figure is shifted and expanded with respect to that of Fig. 2.

tions at a given distance along the x-y line grow more slowly than at the same distance along the x axis. One has to wait about 10% longer for the correlation to reach 99% of equilibrium. One can demonstrate this in a different way by plotting the correlation-function (divided by their final equilibrium value) values of the correlation functions (divided by their final equilibrium value) for correlations along the (1,0) and (1,1) directions at constant time as a function of $\log_2 r$. The results along the (1,1) direction fall below what one would have expected from simply interpolating between the $y=0$ points. This anisotropy is not an artifact of our iteration procedure: The iterated equilibrium (infinite-time) values are isotropic. It is rather a genuine consequence of the fact that the nearest-neighbor correlations grow more rapidly than the next-nearest-neighbor interactions, which, in turn, reflects the fact that this system has only nearest-neighbor interactions. The average domain is somewhat larger measured along the x axis than in any other direction.

Equation (4.13) and our results can be viewed from another point of view: the velocity at which domains expand is proportional to $t^{-1/2}$, and, at a given time, is largest along the x direction.

In Fig. 10 we plot $\epsilon(64,0;t)$ for the same values of u_F as plotted for $\epsilon(1,0;t)$ in Fig. 2. Note the shifted time scale in comparing these figures.

Our results yield direct information on the average behavior of the spatial correlations: a global average over all directions. We interpret L (or $2\pi/q_w$) as being the typical size of a domain, while the crossover region for a given time, where correlations grow from near zero to near final equilibrium values, may be thought of as representing the "wall" regions. We have quantitatively examined this range as a function of time and temperature. It is convenient, as in Figs. 6 and 8, to use a logarithmic scale and define this "wall range," for a given t and u_F, as the region between the distance r_1 where the correlations have attained 80% of their equilibrium value and the distance r_2 where they have attained only 20%. We then define the range θ as $\theta=\log_2(r_2/r_1)$. Measuring θ along the x axis (to avoid confusion with anisotropy effects) one finds the results given in Table I. Note that the fact that θ is approximately equal to a constant in time means that the thickness of this partly ordered region increases in the same way as the average domain.

One should not confuse the behavior of quantities averaged over all space, discussed above, with the behavior of a single domain. While, as we have just seen, there is a rather wide range of distances for which (at a given time) the average correlations vary from their equilibrium to their initial values, the individual domains, on the other hand, have fairly narrow walls. We cannot directly calculate the thickness of these walls, but we can estimate its

TABLE I. $\theta=\log_2(r_2/r_1)$, as defined in the text, is given for various times and final temperatures.

t \ u_F	0.42	0.45	0.55	0.84
10	2.2	2.7	2.6	2.4
100	2.3	2.3	2.2	2.3
1000	2.4	2.4	2.4	2.4

value by the following argument: Let us assume that the density n of domain walls per unit length in a particular direction is given by

$$n=(1/w)e^{-\beta E(w)}, \tag{4.14}$$

where w is the width of the wall $E(w)$ is the energy necessary to create it, and $\beta=1/k_BT$. We can then identify $n\simeq(L+w)^{-1}$, where L is the average size of the domain (which we know, as a function of time). A rough estimate for $\beta E(w)$ is $\sim 2Kw$. We can then numerically solve (4.14) for w. Although the results can only be trusted in terms of their order of magnitude, they are nevertheless interesting. We find that the individual walls are quite sharp: At a time $t=10^3$, for example (the domains are about 100 lattice spacings wide at that time), the walls are ~ 10 lattice spacings wide for $u_F=0.42$ and this number decreases slightly as u_F increases, at constant time. As time (and domain size) increases, the thickness of the walls also increases, but only logarithmically, so that, comparatively speaking, the domains become much better defined. This is in keeping with the fact that surfaces are "rough" in two dimensions.

B. Quasistatic structure factor

In Fig. 11 we plot $\tilde{C}(\vec{q},t)$ as a function of $\vec{q}$ for various times for $u_F=0.42$. The main feature, as mentioned earlier, is the development of a sharp central peak. We see then, for wave numbers less than 0.01, $\tilde{C}(\vec{q},t)\gg C_0(\vec{q},t)$ for all times plotted. Using this very good approximation and going to times sufficiently long that $P(\vec{q},t)\approx 4v_F^2$, we reach the regime where (3.1), and the discussion following it, apply. As discussed in MV we can extract the peak contribution $\tilde{C}_p(\vec{q},t)$ and show that the area under the peak is just m_F^2. That is, $\tilde{C}_p(\vec{q},t)$ grows into a Bragg peak as time evolves—just as we expect.

In Fig. 12 we plot q_w, the half-width at half-maximum of $\tilde{C}(\vec{q},t)$, versus time for $u_F=0.42$. The double-logarithmic plot clearly shows that q_w rapidly crosses over to a $t^{-1/2}$ long-time behavior. In Fig. 13 we plot q_w/π versus u_F for various times and see that q_w is a relatively insensitive function of u_F. The most convenient way of presenting our results for q_w and C_m (the peak height) is via the scaling forms, given by (3.12) and (3.13) with $x=\frac{1}{2}$, which turn out to be applicable for times $t>0.5$. In Fig. 14 we plot f_w versus $x=\xi/\sqrt{t}$, where the true correlation length is given[14] by $\xi=1/\ln(e^{2K_F}u_F)$. For fixed u_F and sufficiently long times, we find

$$f_w(0)=0.509 .$$

We see from Fig. 13 that q_w/π shows no critical effects as $T\to T_c$, and

$$f_w(\infty)=0.611 .$$

The x dependence of f_w shown in Fig. 14 can be approximately fitted to the form

$$f_w(x)=f_w(0)[1-gxf_w(\infty)/f_w(0)]/(1+gx) , \tag{4.15}$$

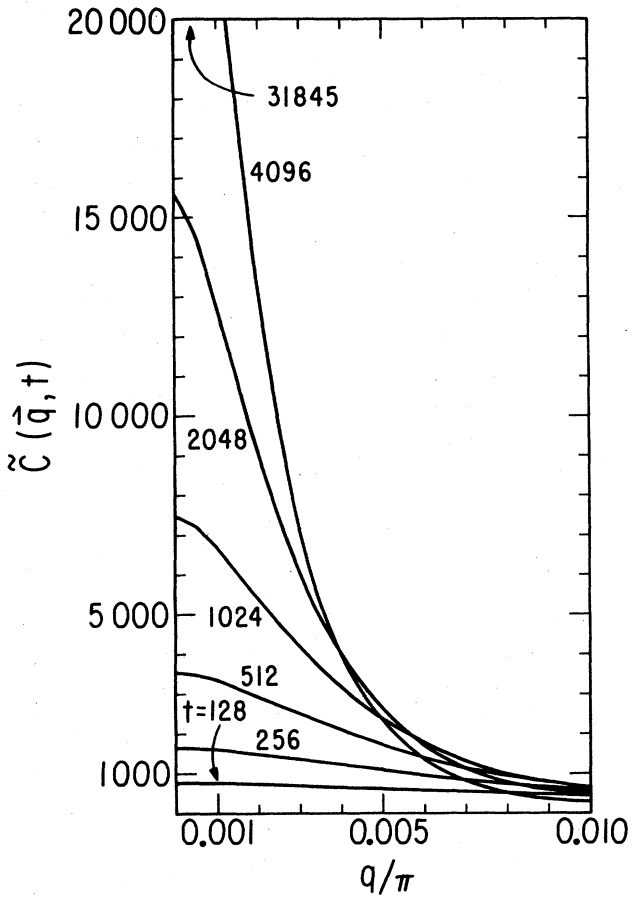

FIG. 11. Structure factor $[\tilde{C}(\vec{q},t)]$ vs q/π for various times after a quench from $u_I=0$ to $u_F=0.42$.

where $g=0.26$.

Similarly, the peak height $C_m(t)$ is accurately given by the scaling form (3.13) for $t>0.5$. The scaling function f_m is plotted versus x in Fig. 15. For fixed $u_F>u_c$, we find, for $t\to\infty$, that

$$f_m(0)=6.718 .$$

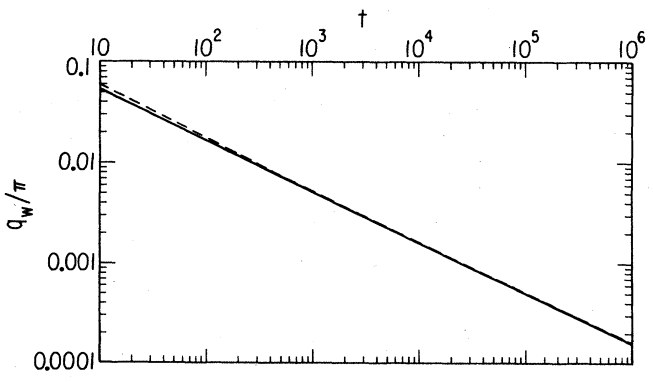

FIG. 12. Double-logarithmic plot of q_w/π vs times t for $u_F=0.42$. The solid curve corresponds to the result $q_w/\pi=(0.509/\pi)t^{-1/2}$ and the dashed curve corresponds to the RG result.

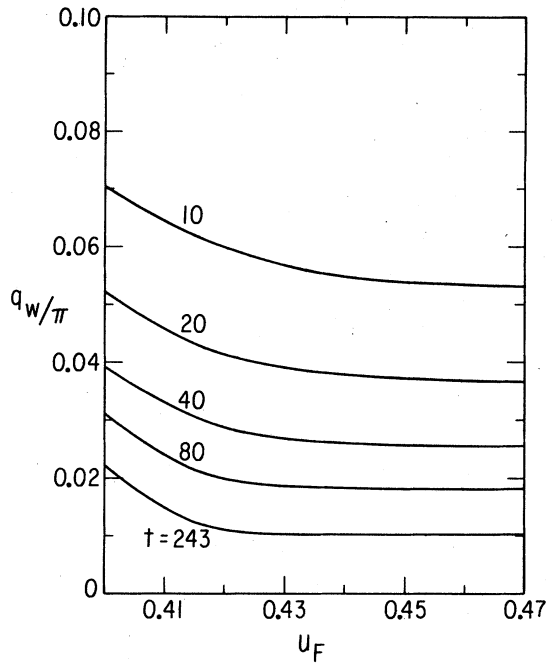

FIG. 13. Half-width q_w/π vs u_F for various times t.

A more interesting result concerns the behavior of $C_m(t)$ near T_c. If we determine $C_m(t)$ for $T=T_c$, we find, for longer times,

$$C_m(t)=4.46t^{0.875}\ . \tag{4.16}$$

This physically sensible result that $C_m(t)$ be finite at T_c for all finite times requires, via (3.13), that

$$f_m(x)=f_0x^{1/4} \tag{4.17}$$

for large x. We find numerically that $f_0=5.87$. The result (4.16) for $C_m(t)$ at T_c has a straightforward interpretation: If the system is in equilibrium at $T=T_c$, then $\tilde{C}(\vec{q})\sim q^{-2+\eta}$ for small wave numbers. For quenches to T_c, the smallest wave numbers that have had a chance to equilibrate in time t after the quench are of order $L^{-1}(t)$, and we expect, therefore,

$$\tilde{C}(\vec{0},t)\sim L^{2-\eta}\sim t^{1-\eta/2}=t^{7/8}\ , \tag{4.18}$$

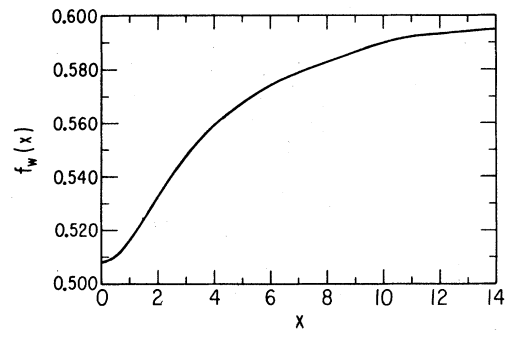

FIG. 14. Scaling function $[f_w(\xi/t^{1/2})]$ for q_w, defined by (1.4), vs $x=\xi/t^{1/2}$.

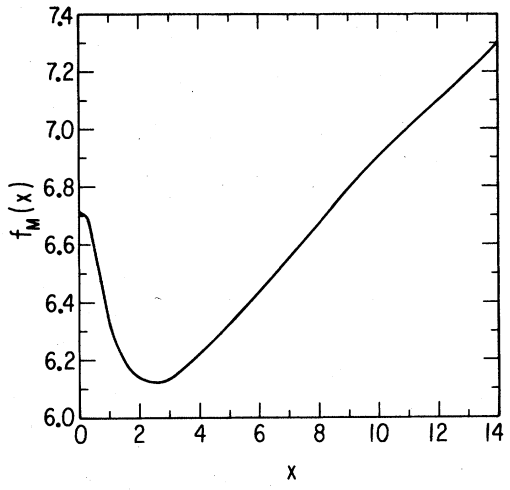

FIG. 15. Scaling function $[f_m(\xi/t^{1/2})]$ for C_m, defined by (1.5), vs $x=\xi/t^{1/2}$.

in agreement with (4.16).

While the presentation of our results for q_w and C_m is most natural in terms of the scaling forms, other types of analysis present themselves. Power-law fits over various limited time ranges will lead to results for effective exponents and amplitudes. If, for $u_F=0.6$, we carry out power-law fits for $0.2<t<1.2$, we obtain

$$q_w/\pi=0.165t^{-0.64}\ , \tag{4.19}$$

$$C_m=6.4t^{0.81}\ . \tag{4.20}$$

Clearly, if one extends the fitted region, the exponents will evolve to -0.50 and 1.0. In particular, if we fit q_w/π to a form Bt^{-x} for various time ranges, we can determine B as a function of u_F (x will be very close to $\frac{1}{2}$ for $t>1$ and $u_F\neq u_c$). Typical results for B are shown in Fig. 16 for fits to two different time ranges. Clearly, B is very sensitive to the time-interval fit.

It is tempting to interpret these results in light of the controlled-growth MC experiments discussed in Ref. 12. In these simulations one begins with a domain area A_0, composed of "up" spins, say, in a sea of "down" spins, and finds that the area A shrinks with time according to $A(t)=A_0-\gamma t$, in agreement with the Cahn-Allen theory. There has been interest in the temperature dependence of γ. Sahni *et al.*[12] find that γ increases as T_F is lowered below T_c and finally saturates for $T/T_c\leq 0.6$. One might suppose that $\gamma^{-1/2}$ is related to B plotted in Fig. 16. Indeed, there is a qualitative similarity—in that γ and B^{-2} increase as T_F is lowered. From our own work, however, we see that B is strongly dependent on the time range studied, and we expect that the detailed temperature dependence of γ is rather strongly tied to the geometry of the growth experiment studied.[29] In a similar fashion we expect γ to depend on the type of dynamics (Glauber or Kawasaki) used and, therefore, not to be a very "universal" quantity.

We turn now to a discussion of the shape function $F(\vec{x},y)$ defined by (3.9) with $\vec{x}=\vec{q}/q_w$ and $y=q_w\xi$. Before we can accurately extract $F(\vec{x},y)$ from our iterated

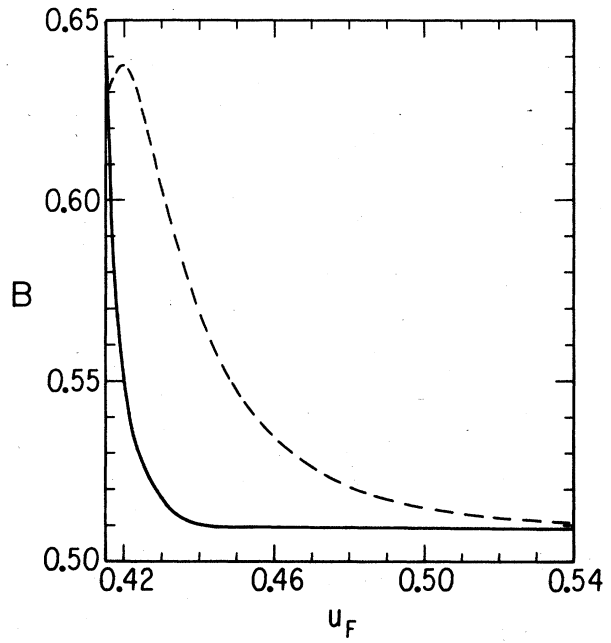

FIG. 16. Quantity B, resulting from fits for $q_w(\xi,t)$ to the form $Bt^{-1/2}$ over different time intervals, vs u_F. The solid curve corresponds to fitting over the time range of 81 to 4 700 000. The dashed curve corresponds to fitting over the time range of 10 to 110.

solution for $\tilde{C}(\vec{q},t)$, there is one complicating technical problem we must discuss.

In solving the recursion relations of the type given by (2.38) it is possible to pick up extraneous and small oscillatory contributions (as discussed in Ref. 5 and MV) associated with the time- and space-rescaling factors. As a trivial example, a recursion relation

$$C(t)=C(\Delta t)$$

will possess solutions of the form

$$C(t)=C_0+C_1\cos(\omega_0 \ln t)+C_2\sin(\omega_0 \ln t)\,, \tag{4.21}$$

where

$$\omega_0=2\pi n/\ln\Delta\,, \tag{4.22}$$

and n is an integer. In particular, we find that the shape function shows such behavior. A direct numerical determination of $F(\vec{x},y)$ for $u_F=0.42$ and times $t=1024$ to 10^6 shows that there is a small oscillatory contribution with precisely the frequency $\omega_0=2\pi/\ln\Delta$. This is clearly an artifact of the choice of the rescaling factor, $b=2$. We can easily identify the components corresponding to C_1 and C_2 in (4.21). We find that the oscillatory component is approximately 5% of the time-independent component. Henceforth we refer only to the uniform component of $F(\vec{x},y)$ in our analysis. The subtraction of the oscillatory terms is achieved by carrying out a three-parameter fit to the form (4.21) (at constant $\vec{x}$ and y). We find that the uniform contribution to $F(\vec{x},y)$ that we extract is independent of the fitting procedure (time range fit, etc.) to better than 1%.

The first question one can ask is how quickly in time does the scaling form (3.8) become appropriate? We find that it takes considerably longer for $F(\vec{x},y)$ to become independent ($t\gtrsim 5$) than it does for q_w to settle into its $t^{-1/2}$ behavior. This is not too surprising since it takes a while for the tail of $F(\vec{x},y)$ (the larger $|\vec{x}|$ values) to rise above the background, and, of course, it is the larger values of $|\vec{x}|$ which become time independent less rapidly.

We have calculated $F(\vec{x},y)$ as a function of u_F for $0.42\le u_F\le 1$ in steps of 0.01 and find *no* appreciable dependence on y to better than 1% accuracy. A plot of $F(\vec{x})=F(\vec{x},0)$ for $\vec{x}$ in the (1,1) direction coincides, over the region of x shown, with that for the angularly averaged quantity $F(x)$ shown in Fig. 17.

For small x, $F(x)$ is isotropic, and Gaussian,

$$F(\vec{x})\sim e^{-ax^2}\,, \tag{4.23}$$

and we obtain numerically that $a=2.37$. For large x we expect

$$F(\vec{x})\sim |\vec{x}|^{-p}\,, \tag{4.24}$$

and we find for $q_x=q_y$ and $4<x<12.5$ that $p\sim 4.4$.

It turns out in this case, however, to be important to study the angular dependence of $F(\vec{x})$. In Fig. 18 we plot $F(\vec{x})$ versus the angle θ that $\vec{x}$ makes with the x axis, for

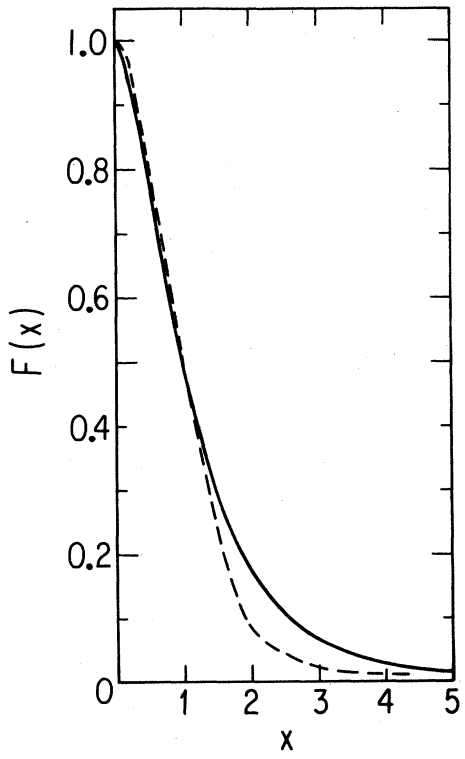

FIG. 17. Shape function $[F(q/q_w)]$, defined by (4.25), vs $x=q/q_w$. The solid lines are the RG calculations. The dashed curve is taken from Ohta *et al.* in Ref. 2.

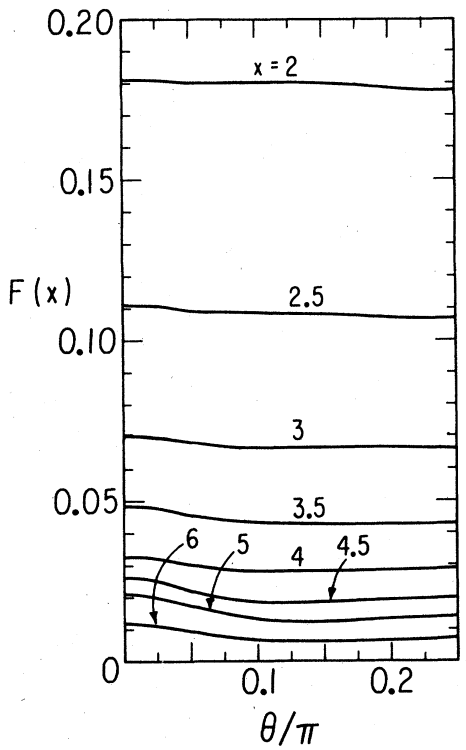

FIG. 18. Shape function $[F(\vec{q}/q_w,q_w\xi)]$, defined by (1.3), vs the angle θ labeling the direction in $\vec{q}$ space, divided by π.

fixed $|\vec{x}|$. We see from the results that $F(\vec{x})$ dies off more slowly in the $\theta=0$ direction. Thus, for larger values of $|x|$, $F(\vec{x})$ is anisotropic and, we believe, gives information about the basic growth pattern in the system. In particular, we see that $F(\vec{x})$ is elongated along the (1,0) direction, in agreement with the analysis in coordinate space that growth proceeds through a "hopping" between nearest neighbors.

In Fig. 17 we have plotted the angularly averaged shape function

$$F(x)=\int_0^{2\pi}\frac{d\theta}{2\pi}F(\vec{x})\ . \tag{4.25}$$

For comparison we have also plotted the shape function found in Ref. 2 normalized such that the points at $x=0$ and 1 (the maximum and half maximum) agree with our definitions. The results are rather similar except in the region $1.5<x<3$. The large-x behavior of the averaged $F(\vec{x})$ varies as x^{-p} with $p=3.04$. This is in reasonable agreement with Perod's law and Ref. 2 where $p=d+1=3$ in two dimensions.

It is our opinion that the MC data is sufficiently poor that direct comparisons for $F(\vec{x})$ are not meaningful. Determinations of the large-x behavior and the exponent p seem somewhat more reliable. We have analyzed the data in Ref. 10 and find $p=2.9$. A value of $p=2.7\pm0.1$ is reported in Ref. 11. The error, it seems to us, is larger than the 0.1 quoted, and thus there is rough agreement between the various determinations of p.

V. DISCUSSION

We have presented in this paper a detailed microscopic theory for the growth of order in an unstable, degenerate system with no conservation laws. The theory agrees quantitatively with Monte Carlo simulations in direct comparisons with no adjustable parameters, and produces all of the expected qualitative features of the growth process. We also have found new results concerning the scaling behavior of q_w, C_m, and $\epsilon(1,0;t)$ which elucidate the role of temperature in the growth process. It will be very interesting to find out if associated shape functions, f_w, f_m, f_ϵ, and F, match with detailed numerical and experimental investigations of systems of this type. We are left with two main questions. First, how sensitive are our major results to the various approximations and parametrizations we have made in our study of the spin-flip kinetic Ising Model? Second, how model dependent are these results?

The most important results we have derived are the scaling equations. Of these, the scaling equation for the structure factor itself was previously known[1] and verified by Monte Carlo simulations. The existence of such a form follows quite generally from the recursion relations of the form (2.38), regardless of any parametrizations later introduced for C_0 and P. The other scaling relations are new. They should be tested by further Monte Carlo simulation. These scaling forms are obtained under the same very general assumptions as that for $\tilde{C}(\vec{q},t)$, in addition to the assumption that Δ is independent of T_F. A sign of a temperature-dependent Δ would be a weak violation of these scaling relations [but not for $\tilde{C}(\vec{q},t)$] for u_F near u_c.

Passing on to the numerical results, the exponents $x=\frac{1}{2}$ and $y=dx$ depend only on the very general assumptions discussed above, as well as the value of Δ at $T=0$ ($\Delta=0.25$). These results, therefore, are also parametrization independent. Our qualitative results (general shape of real-space correlations, area under the central peak, etc.) are also completely general.

The main possible consequence of a change in the determination of λ and λ_1 (or the introduction of additional characteristic times) might be a change in the time scale by a constant, possibly temperature-dependent factor. This is of no great concern (since α^{-1}, our unit of time, is arbitrary), except that it might have to be taken into consideration when comparing our results with future Monte Carlo simulations. Similarly, the determination of the shape functions (as opposed to their existence) might be subject to quantitative changes due to a more careful analysis of C_0 and P.

There are two sets of technical improvements we can carry out to improve our treatments of C_0 and P. The first is the inclusion of larger-$|\vec{m}|$ terms in C_0 [see (2.30)], and the second is a more sophisticated parametrization of the time dependence of the short-range quantities $P(\vec{q},t)$ and $\epsilon_0(\vec{m};t)$ (so as, for example, to be able to include higher-order time derivatives). We will discuss the incorporation of both of these refinements into the formalism in a planned future publication. The main point of interest is the question of numerical convergence

of the results. As explained above, neither qualitative changes nor changes in the exponents should be expected.

What, besides questions of convergence, etc., can go wrong with our theoretical approach here? The main theoretical problem that could develop in the approach we have proposed here is that there might exist additional dynamical variables whose correlations persist to very long times and distances. If such a variable exists, then the simple self-similarity given by (3.1) must be extended to include rescaling of this variable, in addition to αt and ξ. It does not appear that such a variable exists in the problem we have studied here, but it undoubtedly exists in other problems. The clearest example is the role of mode-coupling terms in the problem of phase separation of fluids.

It seems rather clear that the single-spin-flip kinetic Ising model is almost ideal for studying this problem. While it includes all of the essential features of the problem, it is extremely simple. One should now ask how sensitive our results are to extensions and generalizations of the model. Several simple questions come to mind. How sensitive are $f_w(x)$, $f_m(x)$, $f_\epsilon(x)$, and $F(\vec{x},y)$ to changes in the flipping probability $W_i[\sigma]$? We expect the exponents x and y to be insensitive to the choice of $W_i[\sigma]$. A questionable term very relevant to direct comparison with experiment is the temperature dependence of the flipping rate α which we have set to 1 for all temperatures here. Our work here indicates that the appropriate scaling variable will be $\xi/\sqrt{\alpha t}$, where one includes the temperature dependence of α. A somewhat deeper question concerns the nature of universality classes. In critical phenomena it would be sufficient to compare dynamical models where the order parameter is a nonconserved Ising-type scalar without mode coupling to establish the basic dynamic universality class. Thus a single-spin-flip Ising ferromagnet should be in the same critical dynamic universality class as the spin-exchange antiferromagnet. In the quench case, it is a reasonable hypothesis that these two systems share the same scaling behavior. It has been rather well documented[1] that they both satisfy a Cahn-Allen growth law. Do they share the same scaling functions $f_w(x)$, etc.? A detailed comparison has not been carried out.

Unlike critical phenomena it seems possible that the underlying lattice may have an influence on the asymptotic growth process. That is, $F(\vec{x})$ may not be isotropic for sufficiently large $|\vec{x}|$. The angular dependence of $F(\vec{x})$ may contain useful information about the growth and shape of domains.

An interesting issue is the inclusion in our formalism of conservation laws. As we mentioned in the Introduction, preliminary work on the case where the order parameter is conserved has already been reported.[4] We are continuing work in this area (in particular, on the determination of Δ for the antiferromagnetic spin-exchange model).

ACKNOWLEDGMENTS

This work was supported by the National Science Foundation under Grant No. DMR-80-20609 and by the Microelectronics and Information Sciences Center at the University of Minnesota. We are grateful to Scott Anderson and Dr. Fu-chun Zhang for a critical reading of the manuscript.

[1]The recent review by J. D. Gunton, M. San Miguel, and P. S. Sahni [in *Phase Transitions and Critical Phenomena,* edited by C. Domb and J. Lebowitz (Academic, New York, 1983), Vol. 8], gives a thorough discussion of this area up to 1982. See also J. D. Gunton, J. Stat. Phys. **34**, 1019 (1984).

[2]For long times the problem can be approached from the point of view of the behavior of a random array of interfaces. See T. Ohta, D. Jasnow, and K. Kawasaki, Phys. Rev. Lett. **49**, 1223 (1983); K. Kawasaki and T. Ohta, Prog. Theor. Phys. **68**, 129 (1982), and references therein.

[3]G. F. Mazenko and O. T. Valls, Phys. Rev. B **27**, 6811 (1983), referred to in the text as MV.

[4]G. F. Mazenko and O. T. Valls, Phys. Rev. Lett. **51**, 2044 (1983).

[5]G. F. Mazenko, Phys. Rev. B **26**, 5103 (1982).

[6]The more systematic treatment of the conserved case is currently being developed.

[7]S. M. Allen and J. W. Cahn, Acta Metall. **27**, 1085 (1979).

[8]For the dynamical operator we use (Sec. II), one has $t=t_{\rm MCS}/[1+\tanh(2K_F)]$, where $t_{\rm MCS}$ is the time in Monte Carlo steps per spin, and K_F is the coupling characterizing the final state.

[9]P. S. Sahni, G. Dee, J. D. Gunton, M. K. Phani, J. L. Lebowitz, and M. H. Kalos, Phys. Rev. B **24**, 410 (1981).

[10]A Guinier and G. Fournet, in *Small Angle Scattering of X-Rays* (Wiley, New York, 1955).

[11]K. Kaski, M. C. Yalabik, J. D. Gunton, and P. S. Sahni, Phys. Rev. B **28**, 5263 (1983).

[12]P. S. Sahni, G. S. Grest, and S. A. Safran, Phys. Rev. Lett. **50**, 60 (1983); P. S. Sahni and G. S. Grest, J. Appl. Phys. **53**, 8002 (1982).

[13]K. G. Wilson, Phys. Rev. B **4**, 3174 (1971).

[14]M. E. Fisher and R. J. Burford, Phys. Rev. **156**, 583 (1967), W. J. Camp, *ibid.* B **7**, 3187 (1973).

[15]G. F. Mazenko, J. Hirsch, M. J. Nolan, and O. T. Valls, Phys. Rev. B **23**, 1431 (1981).

[16]G. F. Mazenko and O. T. Valls, in *Real Space Renormalization,* edited by J. M. J. vanLeeuwen and T. W. Burkhardt (Springer, Berlin, 1982).

[17]C. N. Yang, Phys. Rev. **85**, 808 (1952).

[18]S. Bradlow and G. Mazenko (unpublished).

[19]G. F. Mazenko and O. T. Valls, Phys. Rev. B **24**, 1404 (1981).

[20]G. F. Mazenko and O. T. Valls, Phys. Rev. B **26**, 389 (1982).

[21]E. Barouch, B. M. McCoy, and T. T. Wu, Phys. Rev. Lett. **31**, 1409 (1973).

[22]H. Tarko and M. E. Fisher, Phys. Rev. B **11**, 1217 (1975).

[23]B. Kaufmann and L. Onsager, Phys. Rev. **76**, 1244 (1949).

[24]This operator was introduced in Ref. 15 and was studied in Refs. 16, 19, 3, and 5. Note that one must divide the minimal coupling $W_i[\sigma]$ by $1+a_F$ to obtain a properly normalized probability distribution. See these earlier references for a fuller discussion of the model studied.

[25]G. F. Mazenko, M. J. Nolan, and O. T. Valls, Phys. Rev. B **22**, 1263 (1980).

[26]See, for example, P. C. Hohenberg and B. I. Halperin, Rev. Mod. Phys. **49**, 435 (1977). For a discussion of the connection between the continuum and lattice-dynamical models, see G. F. Mazenko and O. T. Valls, Phys. Rev. B **24**, 1419 (1981).

[27]A. Sadiq and K. Binder, Phys. Rev. Lett. **51**, 674 (1983); (unpublished).

[28]Two measures of the reliability of this data are (i) $\epsilon(1,0; t=0)=-0.008$ (which is zero exactly), and (ii) the average magnetization is less than 0.023 in magnitude for all times sampled (this should be zero for all times in an infinite system).

[29]Also see the work of M. Grant and J. D. Gunton (unpublished).